RSC Advances

ROYAL SOCIETY OF CHEMISTRY

www.rsc.org/advances

Graphical Abstract

A newly designed duly structurally characterized quinazoline based ratiometric chemosensor (L) senses Al^{3+} ions as low as 1.48 nM selectively through the internal charge transfer (ICT) and chelation enhanced fluorescence (CHEF) processes in water/DMSO (9/1, v/v) medium over other competitive ions and this non-cytotoxic probe (L) is also applicable in living cell staining.

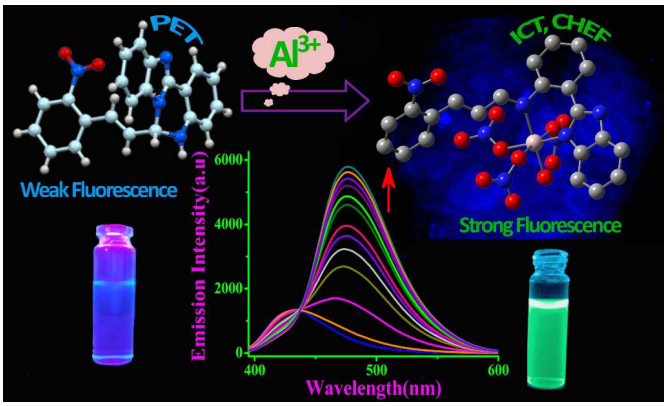

Cite this: DOI: 10.1039/c0xx00000x

www.rsc.org/xxxxxx

ARTICLE TYPE

A quinazoline derivative as quick-response red-shifted reporter for nanomolar Al^{3+} ions and applicable to living cell staining†

*Manjira Mukherjee,[a] Buddhadeb Sen,[a] Siddhartha Pal,[a] Samya Banerjee,[b] Somenath Lohar[a] and Pabitra Chattopadhyay[a]**

Received (in XXX, XXX) Xth XXXXXXXXX 20XX, Accepted Xth XXXXXXXXX 20XX
DOI: 10.1039/b000000x

A newly synthesized and structurally characterized quinazoline derivative (**L**) acts as a quick-response chemosensor for Al^{3+} ions with a high selectivity in water /DMSO medium over other metal ions. In presence of Al^{3+} ions, **L** shows a red shifted fluorescence enhancement ratiometrically due to the internal charge transfer (ICT) and chelation enhanced fluorescence (CHEF) through inhibition of photoinduced electron transfer mechanism. This probe (**L**) detects Al^{3+} ions as low as 1.48 nM in 100 mM HEPES buffer (DMSO/water : 1/9, v/v) at biological pH within a very short responsive time (15-20 s). **L** was further applied for biological imaging to validate it's utility as a fluorescent probe for monitoring Al^{3+} ions in living cells, and exhibited its value in practical applications such as environmental and biological systems.

Introduction

Recently, the development of novel quick-response chemosensors of biologically active metal ions of trace level remains an active research field because of their potential applications in life sciences, medicine, chemistry and biotechnology.[1] The most abundances trace elements in the earth's crust (8.3% by weight) and extensively used in our daily life and several types of industries,[2] results in an increase in the Al^{3+} concentration in food. Aluminium compounds are also frequently utilized as pharmaceutical drugs and cosmetics including antiperspirant in human and veterinary medicine.[3] But aluminium salts are neurotoxic and are suspected to induce Parkinsons' disease and senile dementia, commonly known as Alzheimer's disease, and even it induces geno-toxic and inhibits the repair of radiation-induced lesions in human peripheral blood lymphocytes.[4] After absorption, aluminium is generally distributed and accumulated to all tissues in humans and animals, which give rise to colic, rickets, gastrointestinal problems, interference with the metabolism of calcium, extreme nervousness, anemia, headaches, decreased liver and kidney function, memory loss, speech problems, softening of the bones, aching muscles; and even threat of the cancer of lung as aluminum is alleged to obstruct the respiratory chain by interfering the functioning of iron-sulfur proteins.[5] Thus , the World Health Organization (WHO) advices an average daily human intake of Al^{3+} of around 3-10 mg kg^{-1} and the tolerable weekly dietary intake as 7 mg kg^{-1} body weight.[6]

Considering the above reality, it is clearly understandable that the detection of aluminium ions is indispensable in managing its concentration levels. Lack of spectroscopic characteristics and poor coordination ability of Al^{3+} ions[7] have stimulated the efforts to develop the Al^{3+} ion selective fluorescence probe as fluorescence techniques offer significant advantages over other methods.[8-10] Most of the reported Al^{3+} sensors based on single point chelation-enhanced fluorescence(CHEF)/photoinduced electron transfer (PET)/FRET[11] suffer from interference of Fe^{3+} and Cu^{2+} and require tedious synthetic methodology and are less water soluble.[12] However, the ratiometric CHEF based Al^{3+} selective chemosensor is scarce,[13] though the experimental point of view dictates the advantages of the ratiometric fluorescence signaling, which can provide a built-in correction for environmental effects and stability under illumination.[14]

In this present work, we have developed an efficient ratiometric chemosensor, *6-[2-(2-nitro-phenyl)-vinyl]-5,6-dihydro-benzo[4,5]imidazo[1,2-c]quinazoline* (**L**), for the selective sensing of Al^{3+} ions in DMSO-H_2O (1 : 9, v/v) solution based on chelation-enhanced fluorescence mechanism. This simple and easy to synthesize chemosensor (**L**) has high emission yield, excellent photostability and significant fluorescent behaviour in the visible region. Furthermore, the presence of an excess of the other competitive metal ions including all alkali and alkaline earth metal ions do not affect this fluorescence enhancement behaviour of **L** due to the selective formation of **L′-Al** species.

Experimental

Materials and physical measurements

The analytical grade solvents were and the other reagent grade chemicals utilized in this study were purchased from commercial sources and used as received. Elemental analyses (C, H and N) were carried out on a Perkin Elmer 2400 CHN

elemental analyzer. The UV-1800 and Prestige-21 spectrophotometers made by Shimadzu, Japan were used for recording electronic spectra and IR spectra, respectively. ^{1}HNMR and ^{13}CNMR spectra were obtained on a JEOL 400 spectrometer using DMSO−d_6 solution and a Qtof Micro YA263 mass spectrometer was used to record the electrospray ionization (ESI) mass spectra. To measure the pH of the solution a Systronics digital pH meter (model 335) was employed and the adjustment of pH was done using either 50 mM HCl or KOH solution. Steady-state fluorescence emission and excitation spectra were acquired using a Hitachi-4500 spectrofluorimeter. Time resolved fluorescence lifetime measurements were done taking a TCSPC from PTI, USA, using the sub-nanosecond pulsed LED source (370 nm having a pulse width of 600 ps [full width at half maximum]) (from PicoQuant, Germany) operating at a high repetition rate of 10 MHz driven by a PDL 800-B driver, PicoQuant, Germany. LED profile was measured at the respective excitation of 370 nm with a band pass of 3 nm using Ludox as the scatterer. The collected emission from the sample was at a right angle to the direction of the excitation beam keeping magic angle polarization of 54.71 and the resolution of 146 ps per channel. Felix 32 data analysis software in which reduced w2 and weighted residuals serve as parameters for goodness of fit was used to fit the data to multiexponential functions after deconvolution of the instrument response function by an iterative reconvolution technique

The luminescence property of **L** was examined in water: DMSO (9 : 1, v/v) solvent. pH study was done in 100 mM HEPES buffer solution by adjusting pH with HCl or NaOH. *In vivo* study was performed at biological pH ~7.4 using 100 mM HEPES buffer solution. The stock solutions (~ 10^{-2} M) for the selectivity study of **L** towards different metal ions were prepared taking nitrate salts of Na^{+}, K^{+}, Cu^{2+}, Cr^{3+}, Pb^{2+}, Cd^{2+}, Ag^{+}; acetate salt of Mn^{2+}, Zn^{2+}; chloride salts of Co^{2+}, Ni^{2+}, Ca^{2+}, Hg^{2+}, Mg^{2+}, Fe^{3+}, Fe^{2+} sulphate; in water : DMSO (9 : 1, v/v) solvent. In the study of selectivity, the amount of the metal ions was a hundred times greater than that of the probe used. Fluorescence titration with aluminium nitrate was performed in water: DMSO (9:1, v/v) solvent varying the metal concentration 0 to 100 μM and the concentration of **L** was 10 μM.

Preparation of *6-[2-(2-nitro-phenyl)-vinyl]-5,6-dihydro-benzo[4,5]imidazo[1,2-c]quinazoline* (L)

To an ethanolic solution of *2-(2-aminophenyl)benzimidazole* (2.09 g, 10.0 mmol) (25 mL) *2-nitro cinnamaldehyde* (1.77 g, 10.0 mmol) in 25 mL of ethanol was added dropwise at room temperature under nitrogen atmosphere. The resulting mixture was refluxed for 6.0 h. The slight yellow coloured precipitate of the compound (**L**) was collected through filtration after reducing the solvent on slow evaporation. Single crystal of the compound was obtained from the ethanolic solution.

$C_{22}H_{16}N_4O_2$:. Anal. Found: C, 71.94; H, 4.29; N, 15.76; Calc.: C, 71.73; H, 4.38; N, 15.21. ESI-MS: $[M + H]^+$, m/z, 369.1332 (100 %) (calcd.: m/z, 369.1273. IR (KBr, cm^{-1}): $\nu_{NH,}$ 3078.39, $\nu_{CH=N}$, 1631.78. ^{1}H NMR (400Hz DMSO-d6): δ, 7.88-7.86 (m, 2H); 7.63-7.59 (m,3H); 7.52 (t, 1H, J=7.64); 7.46-7.42 (m, 2H); 7.23 (t, 1H, J = 6.88); 7.18-7.09 (m, 3H); 6.88(d, 1H, J=8.4); 6.79 (t, 1H,J=7.64); 6.70 (dd, 1H, J=7.62); 6.51-6.40 (q, 1H, J_1= 15.28, J_2= 7.6). ^{13}C NMR(400Hz DMSO-d6)): δ, 149.09, 145.36, 145.27, 136.75, 134.62, 133.43, 130.83, 130.77, 130.48, 130.22, 129.79, 129.28, 127.21, 126.84, 126.51, 125.44, 119.98, 116.99, 115.33, 113.66, 105.91, 67.91 Yield: 90%.

Preparation of the aluminium (III) complex (L′-Al species)

To a methanolic solution of **L** (368.0 mg, 1.0 mmol) solid aluminium(III) nitrate nonahydrate (375 mg, 1.0 mmol) was added at a time and then the reaction mixture was stirred at ambient temperature for 6.0 h. The resulting solution thus obtained was then kept aside for slow evaporation at room temperature. After a few days, a deep yellow coloured complex was obtained by washing thoroughly with cold methanol and water, and then dried in vacuo.

$C_{22}H_{18}AlN_7O_{12}$: Anal. Found: C, 44.21; H, 3.01; N, 16.96; Calc.: C, 44.08; H, 3.03; N, 16.36. IR (cm^{-1}): ν_{NO3}, 1341. ESI-MS in methanol: $[M + Na]^+$, m/z, 622.1861 (obsd. with 8 % abundance) (calcd.: m/z, 622.0727) where M = $[Al(L')(ONO_2)_3(H_2O)]$. ^{1}H NMR (δ, ppm in dmso-d_6): 8.07(s, 1H); 7.92-7.73 (m, 3H); 7.65-7.62 (m,1H); 7.60 (d, 1H, J = 7.64); 7.51-7.37 (m, 5H); 7.23 (d, 1H, J = 15.28); 7.00 (d, 1H, J = 7.6); 6.84 (d, 1H, J = 7.6); 6.78 (t, 1H, J = 7.64); 6.51-6.42 (q, 1H, J_1= 15.28, J_2= 7.6). ^{13}CNMR (400Hz DMSO-d6)): δ, 152.08, 149.07, 147.31, 144.80, 143.79, 134.45, 133.60, 132.75, 132.11, 130.87, 130.38, 129.50, 127.49, 125.77, 125.34, 123.38, 123.23, 119.62, 119.40, 116.18, 112.75, 111.60.Yield: 75 %.

***X-ray data collection and structural determination*‡**

The single crystals were obtained from the solution of **L** in methanol on slow evaporation. X-ray data were collected on a Bruker's Apex-II CCD diffractometer using MoKα (λ = 0.71069). The data were corrected for Lorentz and polarization effects and empirical absorption corrections were applied using SADABS from Bruker. A total of 8503 reflections were measured out of which 3602 were independent and 1282 were observed [I >2 σ(I)]. The structure was solved by direct methods using SIR-92[15] and refined by full-matrix least squares refinement methods based on F^2, using SHELX-97.[16] All non-hydrogen atoms were refined anisotropically. All calculations were performed using Wingx package.[17] Crystallographic data duly refined are listed in **Table 1**.

Preparation of cell and *in vitro* cellular imaging with L

HeLa and MCF-7 cells were used in this study were maintained in Dulbecco's Modified Eagle's Medium (DMEM), supplemented with 10% fetal bovine serum (FBS), 100 $\mu g.ml^{-1}$ of penicillin, 100 $\mu g.ml^{-1}$ of streptomycin and 2 mM Glutamax at 37 °C in a humidified incubator at 5% CO_2. The adherent cultures were grown as monolayer and passed once in 4-5 days by trypsinizing with 0.25% Trypsin-EDTA. MCF-7 and HeLa cells (4 x 10^4 cells/mm^2), plated on cover slips, were incubated with **L** (10, 5 and 2 μM, 1% DMSO) for 30 min. After washing

with 50 mM phosphate buffer of pH 7.4 containing 150 mM NaCl (PBS), required volumes of aluminium nitrate stock solution in DMSO were added such that the final concentration of aluminium nitrate adjusted to 2.0 μM, 5.0 μM and 10.0 μM (DMSO will be 1%) and incubated for 30 min. The cells were fixed with 4% paraformaldehyde for 10 min at room temperature (RT). After washing with PBS, mounted in 90% glycerol solution containing Mowiol, an anti-fade reagent, and sealed. Images were acquired using Apotome fluorescence microscope (Carl Zeiss, Germany) using an oil immersion lens at 63X magnification. The images were analyzed using the AxioVision Rel 4.8.2 (Carl Zeiss, Germany) software.[18]

Cell cytotoxicity assay

The photo-cytotoxicity of the ligand was studied in MCF-7 cells using MTT assay which is based on the ability of mitochondrial dehydrogenases of viable cells to cleave the tetrazolium rings of MTT forming dark purple membrane impermeable crystals of formazan that could be measured at 540 nm after solubilization in DMSO.[19] Approximately, 10,000 cells were plated in 96 wells culture plate in Dulbecco's Modified Eagle Medium (DMEM) containing 10% FBS (10% DMEM). After overnight incubation at 37 °C in a carbon dioxide incubator, the solution of **L** of various concentrations in 1% DMSO were added to the cells and incubation was continued for 8 h in dark. Again, after replacing the medium with fresh DMEM-FBS and incubation was continued for further 16 h in dark. Finally, a 25 μL of 4 mg mL^{-1} of MTT solution in PBS was added to each well and again incubated for an additional 3 h. After discarding the culture medium, 200 μL of DMSO was added to dissolve the formazan crystals formed, and the absorbance at 540 nm was measured using a BIORAD ELISA plate reader. The cytotoxic effect of **L** was measured from the absorbance ratio of the treated cells and the controls, and non-linear regression analysis using Graph Pad Prism software was used to determine the IC_{50} values.

Results and discussion

Synthesis and characterization

The organic moiety (**L**) was prepared by condensing an ethanolic solution of *2-(2-aminophenyl)benzimidazole* with *2-nitro cinnamaldehyde* in equimolar ratio (**Scheme1**). The physico-chemical and spectroscopic tools, and the single crystal X-ray crystallography for detailed structural analysis support the formulation of **L** as shown in **Scheme 1**. L is soluble in common polar organic solvents and sparingly soluble in water. The peaks obtained in ^1H NMR spectrum and ^{13}C spectrum of **L** have been assigned and these are in accordance with structural formula of the **L** in the solution state (**Figs. S1** and **S2**†). The ESI mass spectrum of the compound in methanol shows a peak at m/z 369.1332 with 100% abundance assignable to $[M + H]^+$ (calculated value at m/z, 369.1273) where M = molecular weight of **L** (**Fig. S3**†). IR spectrum of **L** shows the characteristic stretching of ν_{N-H} and $\nu_{C=N}$ bonds (**Fig. S4**†). An ORTEP view of the probe **L** with the atom numbering scheme is illustrated in **Fig. 1**. The crystallographic data and the bond parameters (selected bond distances and angles) are listed in **Tables 1** and **2**, respectively. The bond lengths reported in **Table 2** indicate that C14-N3 bond distance (1.444 Å) is shorter than to that of C1-N1 (1.448 Å) but both values are shorter than that of C14-N1 (1.458 Å).

To establish the fact of the formation of the **L′-Al** species, the solid state complex was isolated from the reaction of aluminium(III) nitrate and **L** in 1:1 mole ratio in the methanol medium at stirring condition. The complex is soluble in methanol, DMSO and acetonitrile etc. The peaks obtained in ^{1}HNMR spectrum of the complex have been assigned and it is in accordance with structural formula of the complex, **L′-Al** as $[Al(L')(NO_3)_3(H_2O)]$ (**Figs. S5** and **S6**†). IR spectrum of **L′-Al** species shows the characteristic stretching frequency of NO_3 group (**Fig. S7**†). The ESI mass spectrum of the complex in methanol shows a peak at m/z, 622.1861 with 8 % abundance, assignable to $[M + Na]^+$ (calculated value at m/z, 622.0727), where $M = [Al(L')(NO_3)_3(H_2O)]$ (**Fig. S8**†). Here, during the reaction with Al^{3+} ions, a [1,5] sigmatropic-type shift[10d] of **L** occurred prior to metal coordination (**Scheme 2**), giving *in situ* **L′** which behaved as a bidentate neutral ligand to form $[Al(L')(NO_3)_3(H_2O)]$.

The formation of the **L′-Al** species through [1,5] sigmatropic-type shift has also been supported clearly with the help of ^{13}C NMR spectra of the probe, **L** and **L′-Al** species. Here a peak at δ 67.91 (carbon atom marked as 'v' in **Fig. S2**†) attributable to sp^3 carbon atom in **L** is shifted to downfield at δ = 152.08 in the spectrum of **L′-Al** species (*viz*. **Fig. S6**†) due to change of sp^3 carbon to sp^2 carbon by forming imine type carbon (CH=N). Furthermore all the corresponding peaks of the carbon atoms were found present with usual changes, which confirm the presence of **L′** in **L′-Al** species.

Spectral characteristics

Absorption study

The UV-Vis spectrum of **L** showed the characteristic absorption bands at *ca.* 289 nm, (ε, $1.744x10^4$), 300 nm, (ε, $1.64x10^4$) and 345 nm (ε=$1.432x10^4$) attributable to intramolecular π-π* and n-π* transitions. In UV-Vis titration, addition of the solution of Al^{3+} ion to the colourless solution of **L** in DMSO-water (1:9, v/v) HEPES buffer (0.1M, pH 7.4) at 27°C, a new peak appeared at 394 nm due to the formation of blue colour of the resulting solution . The peak in UV region at 345 nm obtained in the absorption spectrum of the probe, gradually decreases with the addition of Al^{3+} ions and, a new peak generates at around 396 nm with a 49 nm red shift through an isosbestic point at 377 nm (**Fig. 2**) due to the formation of the colored Al(III) complex of the probe in the solution state.

Emission study

The fluorescence spectra of **L** displayed a very weak emission at 430 nm (λ_{ex} = 380 nm) (**Fig. S9**†). Gradual addition of Al^{3+} ions (0-15 μM) to **L** (10 μM) causes gradual decrease of the fluorescence intensity at 430 nm with concomitant increase of a new band at *ca.* 476 nm through an isoemissive point at 436 nm (**Fig. 3**). The weak emission at 430 nm of free **L** in DMSO-water (1:9, v/v) medium is attributed to the ICT process and it is established by an experiment where bathochromic shift of

the emission of **L** with increasing solvent polarity was recorded (**Fig. S10**†). **L** undergoes solvent assisted 1,5-σ tropic shift leading to a more conjugated benzimidazole derivative with more chelating environment at the ICT acceptor site (**Scheme 1**).[10d] On gradual addition of Al^{3+} ions to **L** in DMSO-water (1:9, v/v) medium, the red shift of emission from 430 nm to 476 nm was occurred due to the binding of Al^{3+} at the ICT acceptor site (i.e. imine nitrogen end) of the **L**[20] and the coordination of Al^{3+} ions ceased molecular flexibility and vibration out of fluorophore's planarity which gives rise to the emission enhancement at 476 nm through chelation enhanced fluorescence (CHEF) process (**Scheme 2**). The ratiometric enhancement at 476 nm (*ca.* 11.8 times) is in agreement of ten times increase in quantum yield. **L** has a quantum yield of Φ = 0.069 but the emission intensity gradually increases with increase of added Al^{3+} ions. Addition of Al^{3+} ions (10 μM) to **L** (10 μM), the intensity of the emission was increased with the enhancement of fluorescence quantum yield[21] by *ca.* ten times (Φ = 0.708) in ethanol medium, estimated by integrating the area under the fluorescence curves with the equation:

$$\phi_{sample} = \frac{OD_{standard} \times A_{sample}}{OD_{sample} \times A_{standard}} \times \phi_{standard}$$

There was almost no interference for the detection of Al^{3+} even in the presence of 100 equivalent concentration of alkali and alkaline earth metal ions (Na^+, K^+, Mg^{+2}, Ca^{+2}), and 50 equivalent concentration of several transition metal ions (Mn^{+2}, Fe^{+2}, Fe^{+3}, Co^{+2}, Ni^{+2}, Cu^{+2}, Zn^{+2}) (**Fig. S11** and **S12**†). Job's plot analysis (**Fig. 4**) revealed that *in situ* formed **L** yield a 1:1 **L′-Al** species. The binding constant (K, $8.27X10^4$ M^{-1}) was determined from the emission intensity data (**Fig. 5**) using the modified Benesi-Hildebrand equation corresponding to 1:1 stoichiomtry.[22]

$$1/(F_x-F_0)=1/(F_{max}-F_0)+(1/K[C])(1/(F_{max}-F_0)$$

where F_0, F_x, and F_∞ are the emission intensities of organic moiety considered in the absence of Al^{3+} ions, at an intermediate Al^{3+} concentration, and at a concentration of complete interaction, respectively, and where [C] is the concentration of Al^{3+} ions.

The fluorescence average lifetime measurement of **L** in presence and absence of Al^{3+} ion in the water-DMSO (9:1) medium indicates the gradual increase with increase of Al^{3+} ion concentration (**Fig. S13**†). The average lifetimes were calculated to be 7.93 ns for only **L**, 6.23 ns for the mixture of **L:** Al^{3+} (1:0.5) and 4.22 ns for **L**: Al^{3+} (1:1). The strong binding of Al^{3+} with organic moiety reflected from the binding constant value, has played a key role for the selective CHEF in presence of Al^{3+} ion. The radiative rate constant k_r and total non-radiative rate constant k_{nr} of **L** and aluminium(III) complex were calculated using the equations: $\tau^{-1} = k_r + k_{nr}$ and $k_r = \Phi_f/\tau$,[23] and tabulated in **Table S1**. The data clearly show the fantastic increase of the ratio of k_r/k_{nr} from 0.074 for **L** to 2.26 for **L′-Al**, which is playing the key role in the enhancement of the fluorescence through chelation.

^{1}HNMR titration

In order to strengthen the above bonding pathway of Al^{3+} ions with **L**, ^{1}HNMR titration was performed by addition of Al^{3+} ions to the DMSO-d_6 solution of **L** and significant spectral changes were observed during addition of Al^{3+} ions (**Fig. S14**†). After the addition of 1.0 mM Al^{3+} ions to the solution of 1.0 mM **L**, a new peak of imidazolic NH apears at δ = 8.07 ppm with the disappearance of 6-membered N-H. Furthermore the peaks at δ ≈ 7.6, 7.58, 7.16, 7.09, 6.7 corresponding to $H_{b'}$, H_c, H_g, H_i and H_l shifted to δ ≈ 7.9, 7.47, 7.38, 7.23and 6.84 respectively. These significant spectral changes in ^{1}HNMR titration emphasize the mode of chelation of **L** with Al^{3+} ion to form **L′-Al** species in solution state.

Selectivity

The fluorescent response of organic moiety towards the different metal ions were investigated with 100 times concentration of alkali (Na^+, K^+), alkaline earth (Mg^{2+}, Ca^{2+}), and transition-metal ions (Mn^{2+}, Ni^{2+}, Zn^{2+}, Cd^{2+}, Co^{2+}, Cu^{2+}, Fe^{2+}, Fe^{3+}, Cr^{3+}, Hg^{2+}) and Pb^{2+}, Ag^+ (**Figs. S11** and **12**†). It reveals that the probe, **L** has an extraordinary selectivity and specificity to Al^{3+} ion over other competitive cations.

Effect of pH

The fluorescence intensity of **L** was measured at various pH values adjusting the pH using HEPES buffer in presence and absence of Al^{3+} ion. In the absence of Al^{3+} ion, **L** exhibited a fluorescence of weak intensity with pH independency over the pH range 6.0 to 10.0 (**Fig. S15**†). And the fluorescence intensity of the probe (**L**) in presence of Al^{3+} ion is remarkably higher than that in absence of Al^{3+} ion.

Analytical figure of merit

Based on the fluorescence enhancement at 476 nm, the detection limit was calculated from the calibration curve **(Fig. 6**) focusing on the lower concentration region of Al^{3+} ions. The detection limit was estimated using the equation 3σ/S , where S = the slope of the curve and σ_{zero} = the standard deviation of seven replicate measurements of the zero level, The data from this graph indicates that this probe effectively detect Al^{3+} ion at very low level concentration (LOD = 1.48 nM)[24].

Cell Imaging

To explore the utility of the probe (**L**) in biological systems, it was applied to MCF-7 and HeLa cells. Here, Al^{3+} and **L** were allowed to uptake by the cells of interest and the images of the cells were captured by fluorescence microscopy following excitation at ~ 405 nm **(Figs.7** and **S16**†**)**. Additionally, the *in vitro* study showed that the probe, **L** has shown non-cytotoxic nature towards the cells upto 8.0 h (IC_{50} > 50 μM) (**Fig. S17**†). These results indicate that the probe has a huge potentiality for both *in vitro* and *in vivo* application as Al^{3+} sensor as well as imaging in different ways as same manner for live cell imaging can be followed instead of fixed cells.

Conclusion

In conclusion, a new quinazoline derivative (**L**) has been

designed and crystalographically characterized and it behaves as a quick-response Al^{3+} ions selective ratiometric chemosensor through CHEF process in 100 mM HEPES buffer (water/DMSO : 9/1, v/v) at biological pH. All the processes have been evidenced by thorough experimental findings and significant spectral changes in electronic, fluorimetric and ^{1}HNMR titration. This bio-friendly probe is also useful to detect the intercellular Al^{3+} ions in MCF-7 cells. It is also remarkable that this Al^{3+} ions selective CHEF based ratiometric probe associated with red shift is of better-quality compared to the previously reported red shifting fluorescence probes in terms of the detection limit and medium of the detection as here the LOD was found to be is 1.48 nM in green solvent.[13]

Acknowledgements

The authors gratefully acknowledge the financial assistance from Council of Scientific and Industrial Research (CSIR), New Delhi, India. M. Mukherjee wish to thank to UGC, New Delhi, India for offering the fellowships. The authors are thankful to Prof. B. Mukhopadhyay, IISER, Kolkata for providing the facility to record some ^{1}H NMR and ^{13}C NMR spectra and USIC, The University of Burdwan, for the single crystal X-ray diffractometer facility under PURSE program.

Notes and references

[a]*Department of Chemistry, Burdwan University, Golapbag, Burdwan-713104, West Bengal, India, E-mail: pabitracc@yahoo.com*
[b]*Department of Inorganic and Physical Chemistry, Indian Institute of Science, Bangalore, 560012, India*

†Electronic Supplementary Information (ESI) available: See DOI: 10.1039/b000000x/

‡ CCDC 1021032 contains the supplementary crystallographic data for this paper. These data can be obtained free of charge from The Cambridge Crystallographic Data Centre *via* http://www.ccdc.cam.ac.uk/data_request/cif.

1.(a) R.P. Haugland, *The Molecular Probes Handbook: A Guide to Fluorescent Probes and Labeling Technologies*, 10th ed.; Invitrogen: Carlsbad, CA, 2005. (b) A.P. de Silva, H.Q.N. Gunaratne, T. Gunnlaugsson,; A.J.M. Huxley, C. P. McCoy, J.T. Rademacher, T.E. Rice, *Chem. Rev*. 1997, **97**, 1515; (c) S.C. Burdette, S.J. Lippard, *Coord. Chem. Rev*. 2001, **216**, 333; (d) D.T. McQuade, A.E. Pullen, T.M. Swager, *Chem. Rev*. 2000, *100*, 2537.

2.(a) W. S. Miller, L. Zhuang, J. Bottema, A. J. Wittebrood, P. De Smet, A. Haszler and A. Vieregge, *Mater. Sci. Eng A.*, 2000, **280**, 37; (b) R. E. Doherty, *Environ. Forensics*, 2000, **1**, 83; (c) G. Ciardelli and N. Ranieri, *Water Res.*, 2001, **35**, 567; (d) R. Flarend, T. Bin, D. Elmore and S.L. Hemb, *Food Chem. Toxicol.* 2001, **39,** 163; (e) R. A. Yokel, *Food Chem. Toxicol.*, 2008, **46**, 2261.

3. J. L. Greger, *Crit. Rev. Clin. Lab. Sci.*, 1997, **34**, 439.

4.A. Lankoff, A. Banasik, A. Duma, D. Ochniak, H. Lisowska, T. Kuszewski, S. G´o´zd´z and A. Wojcik, Toxicol. Lett., 2006, 161, 27.

5.(a) M. Hemadi, G. Miquel, P.H. Kahn and J.M.E.H. Chahine, *Biochemistry*, 2003**, 42**, 3120; (b) R.B. Martin, J. Savory, S. Brown, R.L. Bertholf and M.R. Wills, *Clin. Chem.*, 1987, **33**, 405; (c) A. J. Roskams and J.R. Connor, *Proc. Nati. Acad. Sci. USA*, 1990, **87**, 9024; (d) M. Cochran, V. Chawtur, M.E. Jones and E.A. Marshall, *Blood***,** 1991**, 77**, 2347; (e) S. Kim, J. Y. Noh, K. Y. Kim, J. H. Kim, H. K. Kang, S.W. Nam, S. H. Kim, S. Park, C. Kim and J. Kim, *Inorg. Chem.,* 2012, **51**, 3597 and refs. therein.

6. B. Valeur and I. Leray, Coord. Chem. Rev., 2000, **205**, 3.

7. K. Soroka, R. S. Vithanage, D. A. Phillips, B. Walker and P. K. Dasgupta, Anal. Chem., 1987, 59, 629.

8. J.R. Lakowicz, *Principles of Fluorescence Spectroscopy*, Springer 2006.

9. (a) A.P. de Silva, D.B. Fox, J.M. Huxley and T.S. Moody, *Coord. Chem. Rev.*, 2000, **205**, 41; (b) B. Valeur and I. Leray, *Coord. Chem. Rev.*, 2000, **205**, 3.

10. (a) S. Sen, T. Mukherjee, B. Chattopadhyay, A. Moirangthem, A. Basu, J. Marek and P. Chattopadhyay, *Analyst*, 2012, **137**, 3975; (b) S. Sen, T. Mukherjee, S. Sarkar, S. K. Mukhopadhyay and P. Chattopadhyay, *Analyst*, 2011, **136,** 4839; (c) U. C. Saha, K. Dhara, 60 B. Chattopadhyay, S. K. Mandal, S. Mondal, S. Sen, M. Mukherjee, S. V. Smaalen and P. Chattopadhyay, *Org. Lett.*, 2011, **13**, 4510; (d) U. C. Saha, B. Chattopadhyay, K. Dhara, S. K. Mandal, S. Sarkar, A. R. Khuda-Bukhsh, M. Mukherjee, M. Helliwell and P. Chattopadhyay, *Inorg. Chem.*, 2011, **50**, 1213; (e) K. Dhara, U. C. 65 Saha, A. Dan, M. Manassero, S. Sarkar and P. Chattopadhyay, *Chem. Commun*., 2010, **46**, 1754; (f) M. Mukherjee, B. Sen, S. Pal, M. S. Hundal, S.K. Mandal, A.R. Khuda-Bukhsh and P. Chattopadhyay, *RSC Advances*, 2013, **3**, 19978.

11. B. Sen, S. Pal, S. Lohar, M. Mukherjee, S.K. Mandal, A.R. Khuda-Bukhsh and P. Chattopadhyay, *RSC Advances*, 2014, **4**, 21471 and references therein.

12.(a) S. M. Z. Al-Kindy, F. E. O. Suliman and A. E. Pillay,m Instrum. Sci. Technol., 2006, 34, 619; (b) J. L. Ren, J. Zhang, J. Qing Luo, X. K. Pei and Z. Xi Jiang, Analyst, 2001, 126, 698; (c) S. M. Ng and R. Narayanaswamy, Anal. Bioanal. Chem., 2006, 386, 1235; (d) Y.-W. Wang, M.-X. Yu, Y.-H. Yu, Z.-P. Bai, Z. Shen, F.-Y. Li and X.-Z. You, Tetrahedron Lett., 2009, 50, 6169.

13.(a) D. Jeyanthi, M. Iniya, K. Krishnaveni and D. Chellappa, *RSC Adv*., 2013, **3**, 20984; (b) J. Hatai, M. Samanta, V. S. Rama Krishna, S. Pal and S. Bandyopadhyay, *RSC Adv*., 2013, **3**, 22572; (c) S. Goswami, S. Paul and A. Manna, *RSC Adv*., 2013, **3**, 25079

14. (a) Z. Xu, Y. Xiao, X. Qian, J. Cui and D. Cui, *Org. Lett*., 2005, **7**, 889; (b) B. Valeur,; and I. Leray, *Coord. Chem. Rev.*, 2000, **205**, 3; (c) S. Sen, S. Sarkar,B. Chattopadhyay, A. Moirangthem, A. Basu, K. Dhara and P. Chattopadhyay, *Analyst*, 2012, **137,** 3335.

15. A. Altomare, G. Cascarano, C. Giacovazzo and A. Guagliardi*, J. Appl. Crystallogr.*, 1993, **26**, 343.

16. G. M. Sheldrick, *Acta Cryst. A*, 2008, **A64**, 112.

17. L.J. Farrugia, *J. Appl. Cryst.*, 1999, **32**, 837.

18. J. L. McClintock and B. P. Ceresa, *Invest. Opthalmol. Vis. Sci.*, 2010, **51,** 3455.

19. S. Banerjee, A. Dixit, R. N. Shridharan, A. A. Karande, A. R. Chakravarty, *Chem. Commun.* **2014**, *50*, 5590-5592.

20. J.R. Lakowicz, *Principles of Fluorescence Spectroscopy*, Springer 2006.

21. W. H. Melhuish, *J. Phys. Chem.*, 1961, **65**, 229

22. H.A. Benesi and J. H. Hildebrand, *J. Am. Chem. Soc.*, 1949, **71**, 2703.

23. N.J. Turro, *Modern Molecular Photochemistry*; Benjamin/ Cummings Publishing Co., Inc.: Menlo Park, CA, 1978, 246.

24. (a)M. Mukherjee ,S. Pal, B. Sen, S. Lohar, S. Banerjee, S. Banerjee and P. Chattopadhyay, *RSC Adv*., 2014, **4**, 27665. 28 (b) S. Pal, B. Sen, M. Mukherjee, K. Dhara, E. Zangrando, S. K. Mandal, A.R. Khuda-Bukhsh and P. Chattopadhyay, *Analyst*, 2014, **139**, 1628

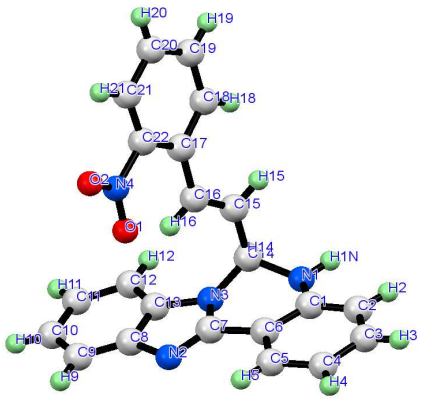

Fig. 1 An ortep view of **L** with atom numbering scheme (50% probability structure.

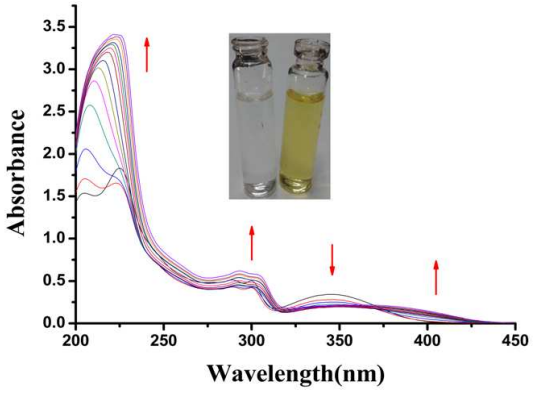

Fig. 2 UV-Vis titration spectra of **L** with Al(III) ions (0, 0.5, 1, 2, 3, 4, 5, 6, 7, 8, 9, 10, 12, 15 µM respectively) in 100 mM HEPES buffer (DMSO/ water: 1/9) at 27 °C.

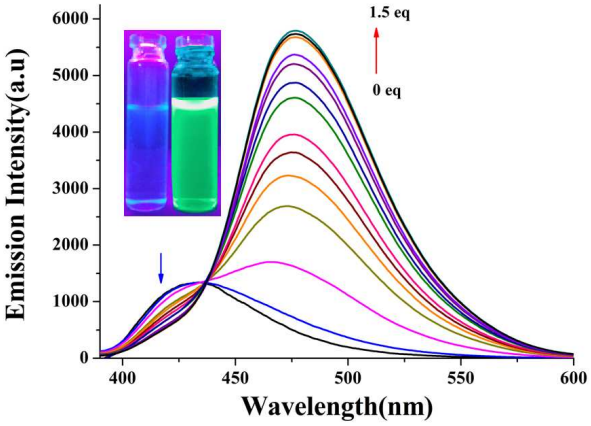

Fig. 3 Fluorescence titration of **L** with incremental addition of Al(III) ions (0, 0.5, 1, 2, 3, 4, 5, 6, 7, 8, 9, 10, 12, 15 µM respectively) in 100 mM HEPES buffer (DMSO/ water: 1/9) at 27 °C.

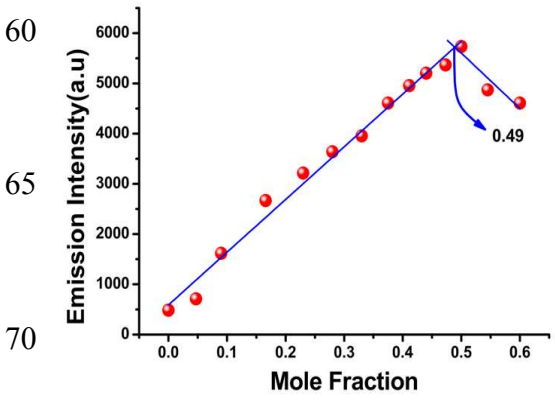

Fig. 4 Job's plot of **L** showing 1:1 stoichiometry.

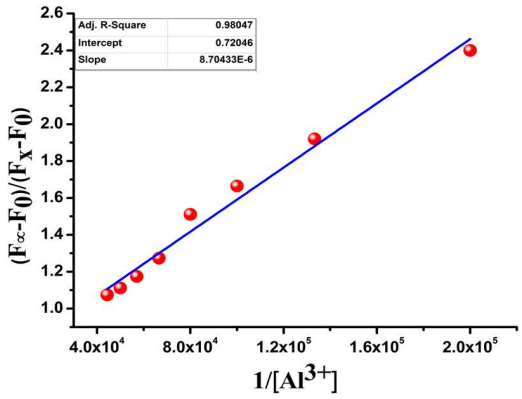

Fig. 5 Binding constant (K) value of 8.27X10^4 M^{-1} for **L** determined from the intercept/slope of the Emission plot.

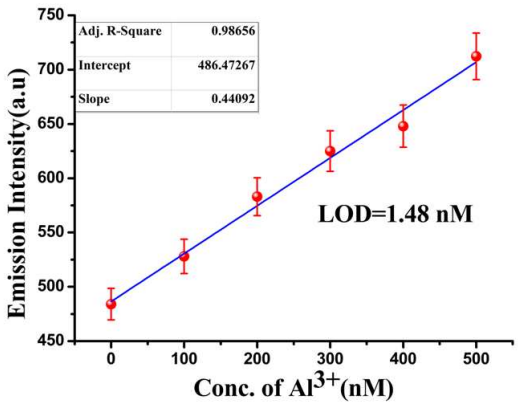

Fig. 6 Calibration curve for the nanomolar range, with error bars for calculating the LOD of Al(III) by **L** in 100 mM HEPES buffer (DMSO/ water: 1/9) at 27 °C.

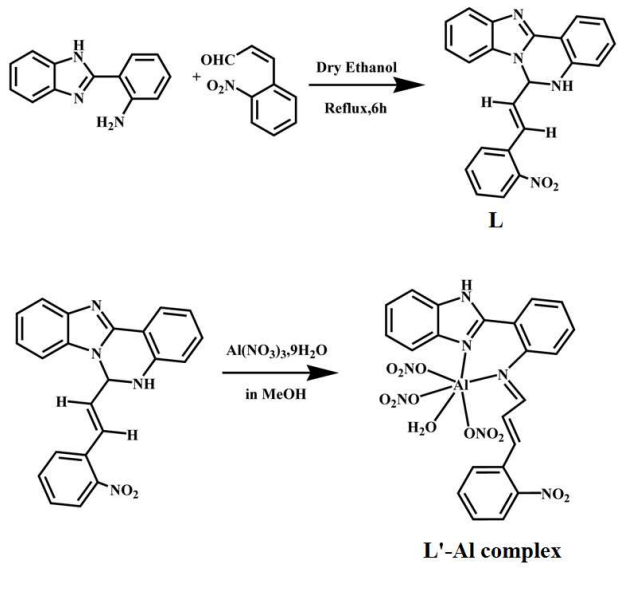

Scheme 1 Schematic representation of synthesis of the probe **L** and the corresponding Al(III) complex.

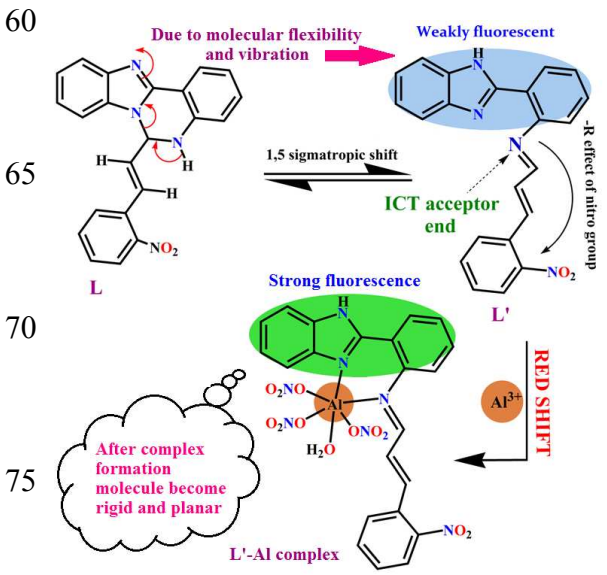

Scheme 2 Probable mechanistic pathway for sensing of Al^{3+} ions.

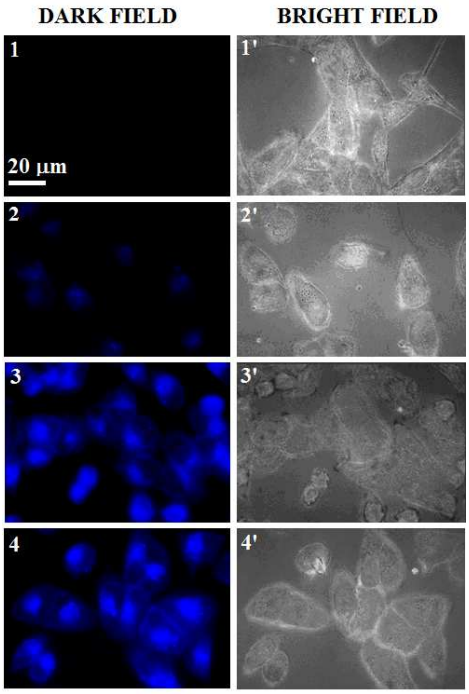

Fig. 7 Fluorescence image of Hela cells (1,1') controll, (2,2') cells were incubated with 0 µM Al^{3+}, (3,3') cells incubated with 5 µM Al^{3+} and (4,4') cells incubated with 10 µM Al^{3+}. All the samples were excited at 380 nm by using a [63 X] objective.

Table 1 Crystal data and details of refinements for **L**

Empirical Formula	$C_{22}\ H_{16}\ N_4\ O_2$
Formula Weight	368.39
Crystal system	monoclinic
Space group	P 21/n
a (Å)	10.390(5)
b (Å)	16.287(5)
c (Å)	11.124(5)
$\alpha = \beta$	90°
γ	105.725(5)
Volume ($Å^3$)	1812.0(13)
Z	4
ρ_{calc} (g/cm^3); µ (mm^{-1})	1.350; 0.090
F(000)	768.0
θ range (deg)	2.380 to19.979°
Reflections collected	1681
Reflections independent	1220
Final R indices [$I > 2\sigma(I)$]	R = 0.10160, wR2 = 0.3523

Table 2 Selected bond distances (Å) and bond angles (°) for **L**

Bond length (Å)	
N1 - C1	1.448(11)
N1- C14	1.458(10)
N2 - C7	1.262(10)
N2 - C8	1.479(12)
N3 - C7	1.301(10)
N3 – C13	1.484(10)
N3 C14	1.444(10)
C15-C16	1.245(9)
Bond angles (º)	
C1 N1 C14	121.1(7)
C7 N2 C8	100.5(8)
C7 N3 C14	128.8(8)
C7 N3 C13	103.3(8)
C14 N3 C13	125.7(8)
C2 C1 N1	123.2(9)